JOURNAL OF MATERIALS SCIENCE 12 (1977) 1988–1993

The solidification behaviour of melts in the system Zn_2SiO_4-Mg_2SiO_4

L. WEBER, E. GRAUER-CARSTENSEN
Anorganisch-Chemisches Institut der Universität Zürich, Switzerland

The melting and solidification behaviour of various compositions across the system Zn_2SiO_4–Mg_2SiO_4 (willemite–forsterite) was studied by means of photoemission electron microscopy, X-ray diffraction and DTA. The results revealed the peritectic type of the phase system instead of the earlier assumed eutectic one. During the formation of willemite solid solutions by rapid solidification of zinc-silicate-rich melts, grain-boundary enrichment of zinc oxide besides magnesium silicate takes place. From melts richer in magnesium silicate, forsterite solid solution forms primarily. The sluggish process of its peritectic decomposition during cooling and the preferred subsolidus formation of zinc silicate give rise to the formation of a ternary non-equilibrium phase assemblage even at slow cooling.

1. Introduction

Earlier studies on the formation of crystalline and glassy phases from melts is such complex silicate systems as Li_2O–MgO–ZnO–SiO_2 [1, 2] are based on the knowledge of the simpler subsystems Li_2O–SiO_2 [3, 4], ZnO–SiO_2 [5, 6]. ZnO–MgO–SiO_2 [7] and Zn_2SiO_4–Mg_2SiO_4 [8]. The latter pseudobinary willemite–forsterite system is only partially known: the limits of the willemite and forsterite solid solutions were investigated by means of solid state reactions at various temperatures [8] while the liquidus relations were only assumed tentatively to represent a eutectic phase diagram.

The present work deals with the melting and solidification behaviour of various compositions across this system. It was undertaken as the continuation of earlier studies in the phase systems Zn_2SiO_4–SiO_2 [9] and ZnO–Zn_2SiO_4 [10] employing photoemission electron microscopy (PhEEM), X-ray diffraction and differential thermal analysis (DTA).

2. Experimental procedure

Powder fractions of reagent grade ZnO, MgO and SiO_2 were intimately mixed in various molar portions corresponding to exact molar ratios of Mg_2SiO_4/Zn_2SiO_4 in steps of 10 mol% Mg_2SiO_4. A conventional thermoanalyser (Mettler, Switzerland) was used for DTA measurements with an upper temperature limit at 1600° C. Exact initial weights (70 mg) of the mixtures were sealed in small platinum capsules (3 mm diameter and 20 mm length) and submitted to heating–cooling cycles at rates of 10, 6 and 2° C min^{-1}, respectively. Since no superheating effects were observed at 10° C min^{-1}, this rate was generally used for DTA peak recording with reasonable sensitivity. α–Al_2O_3 was used as reference material. Experimental details on the arrangements of the specimens and thermocouples, on temperature calibration and peak area evaluation are given elsewhere [11].

In order to study the intergrowth morphologies of the solid phases as grown from the melts, additional samples were produced for ceramaographic examination by PhEEM as follows: Powder mixtures (1 to 2 g) were heated in small platinum crucibles (6 to 7 mm diameter) at 1500 to 1600° C. After melting was complete, the samples were either removed from the furnace and allowed to cool in air rapidly (mode A), or they were cooled slowly (6° C min^{-1}) until about 1300° C and subsequently removed from the furnace (mode B). The surfaces of the samples were then ground and polished to get smooth planes for the examination

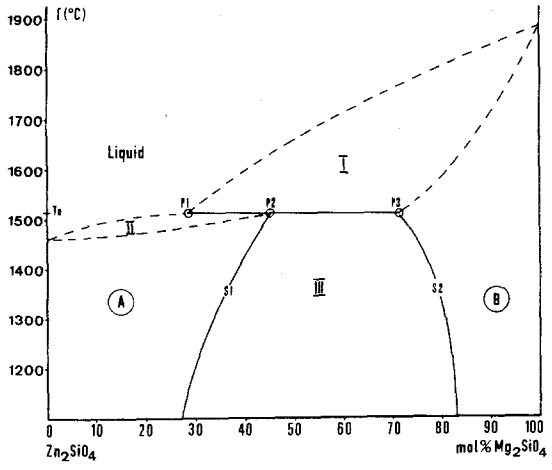

Figure 1 Phase diagram of the system Zn_2SiO_4–Mg_2SiO_4. The solvus lines S1 and S2, and the peritectic line at T_0 including the points P1, P2 and P3 are experimentally determined after [8] and the present work. *A* and *B* are zinc silicate and forsterite solid solutions, respectively. The two-phase fields I, II and III are discussed in the text.

by PhEEM. Details of the method and ceramographic applications of PhEEM were given earlier [9, 10, 12, 13]. All specimens were anlaysed by X-ray diffraction (Cu$K\alpha$ radiation) to identify the crystalline phases present. Chemical analyses by conventional electron microprobe measurements were applied to some selected samples as well.

3. Results and discussion

The present investigation revealed the peritectic character of the willemite–forsterite phase diagram as depicted in Fig. 1. The several experimental results are elucidated in the light of Fig. 1 as follows:

The peritectic temperature T_0 at $1515 \pm 5°$ C was observed by DTA at the onset of strong melting reactions occurring from samples in the compositional range between about 30 and 70%*. The melting temperatures of zinc silicate was earlier reported to be 1512 and 1505° C, respectively [5, 6]. A reliable melting point seems hard to be determined, however, since zinc silicate tends to partial decomposition at elevated temperatures under separation of SiO_2 (cf. below). DTA heating runs in this work yielded even lower temperatures ($\approx 1480°$ C). The DTA peak form indicated a melting region with respect to the temperature rather than a sharp melting process. Additional contents of Mg_2SiO_4 up to about 30% raised the melting point to about T_0.

*Chemical compositions are in mol% Mg_2SiO_4 throughout.

The points P1 and P3 on the peritectic line were established by evaluation of the DTA peak areas (heats-of-fusion) which arise at T_0 due to the formation of partial melts from samples of various compositions. The observed peak areas are proportional to the various amounts of the melts if all samples have the same weight and if the measurements are performed under the same experimental conditions [14, 15, 11].

As a result, the amounts of the melts increase linearly from zero at a sample composition of about (73 ± 3% (P3) to a maximum at about 28 ± 3% (P1) according to the thermodynamic "lever rule" applied on the peritectic tie-line. Between 30 and 5% overall composition of the samples, some smaller non-linear increase of the peak areas was observed due to the compositional change of the zinc silicate solid solutions melting.

The solvus lines S1 and S2 after [8] determine, respectively, the limits of the solid solutions of Mg_2SiO_4 in Zn_2SiO_4 ("phase *A*") and vice versa ("phase *B*"). The observed compositions of P3 after this work (73%) and after [8] (76%) are in satisfactory agreement. The solidus and liquidus boundaries of the two-phase region II (Fig. 1)

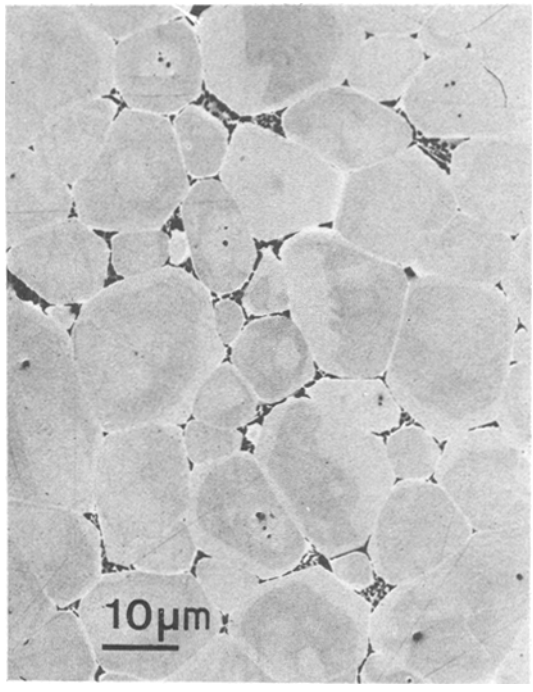

Figure 2 Grains of willemite solid solution (phase *A*, bright) with exsolution of forsterite and enstatite (dark) at the grain boundaries after annealing (see text).

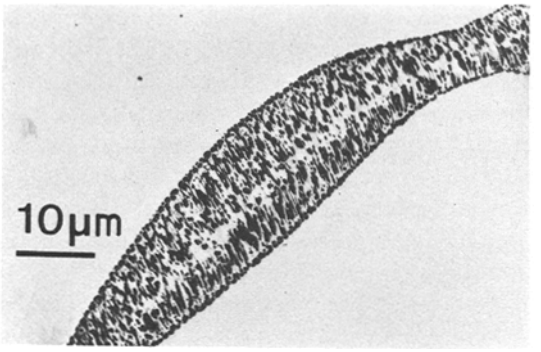

Figure 3 Larger region of the ternary phase morphology between grains of phase *A* (bright). To obtain good brightness contrast the micrograph is overexposed so that phase *A* appears white.

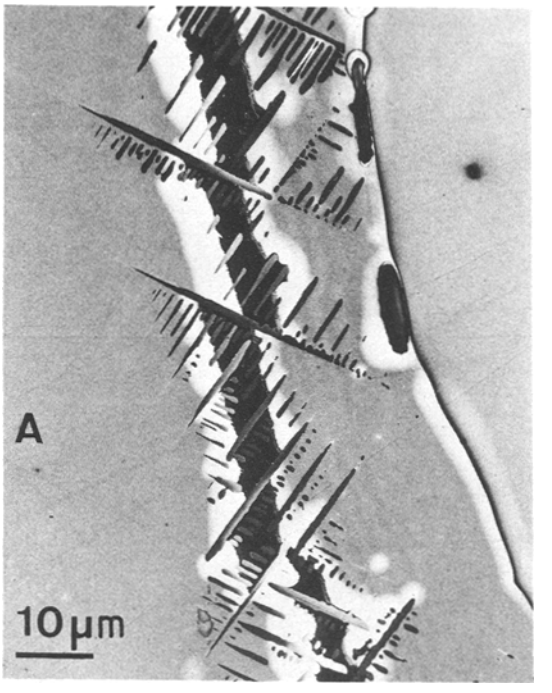

Figure 4 Rapid growth of phase *A* (A) from melts < 45% Mg_2SiO_4 generates a ternary phase assemblage of relatively pure zinc silicate (white), forsterite (black) and zinc oxide (as dendrites) at the grain boundaries.

could not be determined exactly by DTA since this region is very narrow with respect to the temperture.

Some typical morphological features of the solidified melts are presented as PhEEM micrographs in Figs. 2 to 9. They also support the peritectic character of the phase diagram of Fig. 1: From melts in the compositional range up to P1, large grains of zinc silicate solid solutions form during slow cooling (mode B). X-ray diffraction indicates a strong tendency to a distorition of the trigonal lattice with an increased *a*-axis. During subsequent annealing (6 h at 1300° C) the large grains decompose into smaller crystals with again "normal" lattice constants [19]. At the grains boundaries, forsterite and estatite form in accordance with the ternary phase relations [2, 7] due to preferred separation of SiO_2 and MgO from the willemite solid solutions (Figs. 2, 3). PhEEM can not distinguish between forsterite and enstatite since both phases appear dark. Phase identification was obtained, however, by X-ray diffraction*. The separation of MgO and SiO_2 from phase *A* is assumed to be the consequence of preceding loss of little ZnO by volatilization at high temperatures. This effect may also be the reason for the different melting point determinations as reported above. During rapid growth of phase *A* (cooling mode A), ZnO is enriched preferentially besides MgO and SiO_2 in the ambient liquid. The overall composition of the boundary regions of phase *A* is therefore shifted into those ternary fields [7] where willemite, forsterite and zinc oxide are coexistent as seen in Fig. 4. From these boundary regions, forsterite may grow into the interior of the large crystals of phase *A* nucleating partial inhomogeneity (Fig. 5). By additional annealing of these samples (6 to 9 h at 1300° C) the non-equilibrium phases are dissolved and phase *A* becomes homogenous while a similar morphology as in Fig. 2 appears.

From melts with compositions between P1 and P2, primary formation of phase *B* above T_0 takes place. These *B*-crystals have to be dissolved completely below T_0. Figs. 6 and 7 are examples of two different steps of the peritectic decomposition: Fig. 6 illustrates the formation of zinc-silicate-rich clusters while the peritectic reaction proceeds from the boundaries into the interior of the primary *B*-crystals. In Fig. 7, phase *B* has reacted with the melt nearly completely leaving skeleton-like remainders with a composition close to P2 (about 45% Mg_2SiO_4 after microprobe measurements).

*It may be noted in this context that reliable identifications of minor phases at grain boundaries are often difficult since quantitative analyses by electron microprobe need phase areas of about 3 to 5 µm, and X-ray diffraction often suffers from poor crystallinity or from too small amounts of the minor phases present.

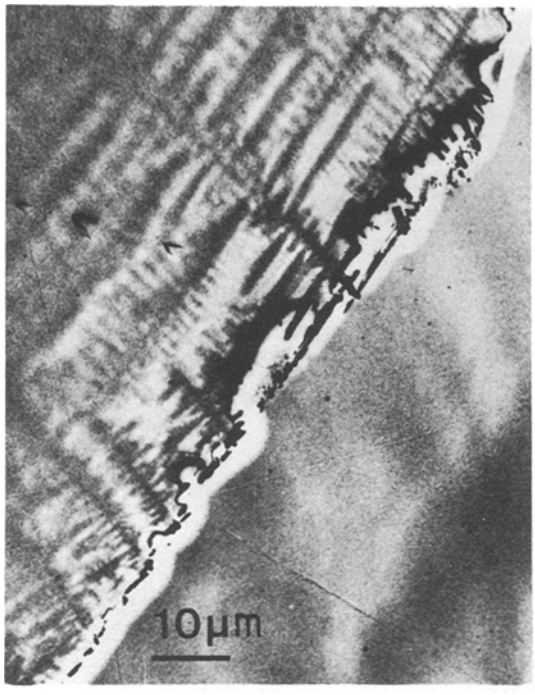

Figure 5 Coarse inhomogeneity of phase A by the growth of dendrites induced by exsolved forsterite (dark) at the grain boundaries.

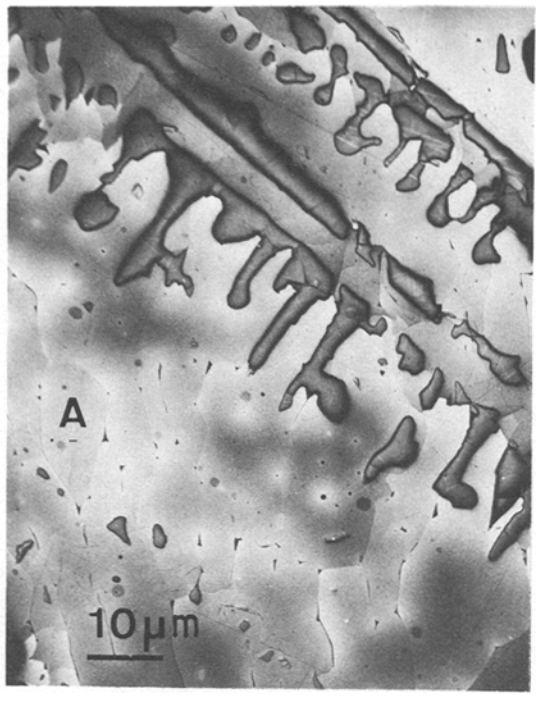

Figure 7 Residual skeleton-like particles of nearly completely decomposed forsterite (dark) and phase A (A).

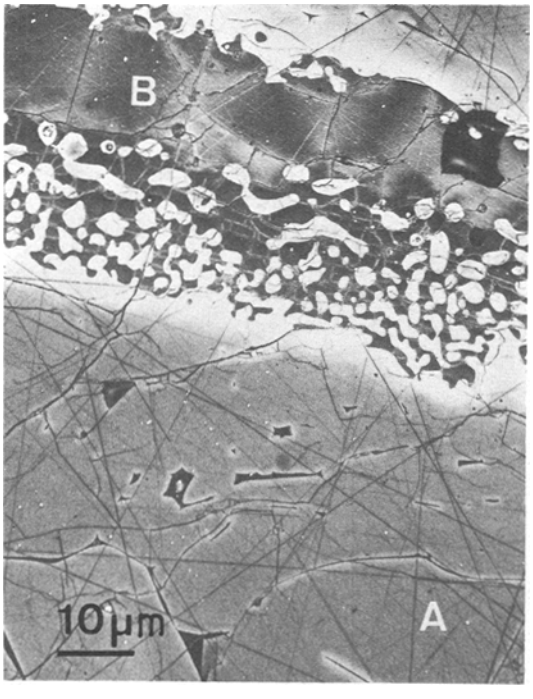

Figure 6 During peritectic decomposition of a primary forsterite crystal (B), zinc silicate rich clusters (bright) are formed. The ambient melt solidifies as phase A since the overall composition is $< 45\%$ Mg_2SiO_4.

The phase morphologies of solidified melts with overall compositions >45% change markedly: Primary phase B is dissolved below T_0 only partially and phase A grows in a lath-shaped, elongated habit (Fig. 8). Low cooling rates (mode B) do not change these principal features but only increase the width of the A-crystals. Phase A does no more crystallize in the stable α-form (willemite) but in an intermediate structural state between the stable α-and the metastable β-state [5, 9]. A similar transitional structure was also observed earlier in the systems Zn_2SiO_2–SiO_2 [9] and ZnO–Zn_2SiO_4 [10]. In all these cases, zinc silicate has to crystallize in a two-solid phase field below the eutectic or peritectic temperature i.e. outisde its solid–liquid field of primary formation.

The mechanism of common phase formation $A + B$ in the two-solid phase field III (Fig. 1) is governed by the growth of phase A, from which SiO_2 is separated rather than MgO as observed by PhEEM (Fig. 8) and semi-quantitative microprobe analysis. Even after slow cooling (mode B) novel formed phase B was not observed. In consequence of this solidification behaviour, the compositions of the intergrain regions of phase A move from the pseudobinary section into the ternary field. This

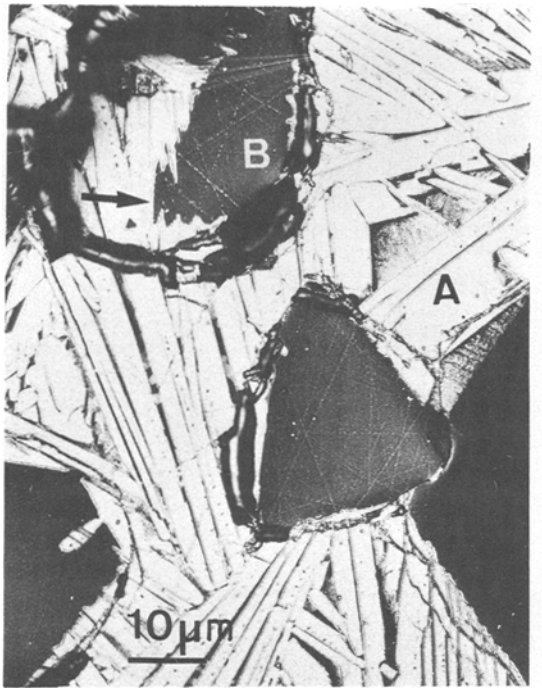

Figure 8 Primary forsterite (B) grown from melts > 45% Mg_2SiO_4 is only partially decomposed below T_0 (see arrow). Lath-shaped growing phase *A* (bright) leaves SiO_2-rich melt (dark) at the boundaries.

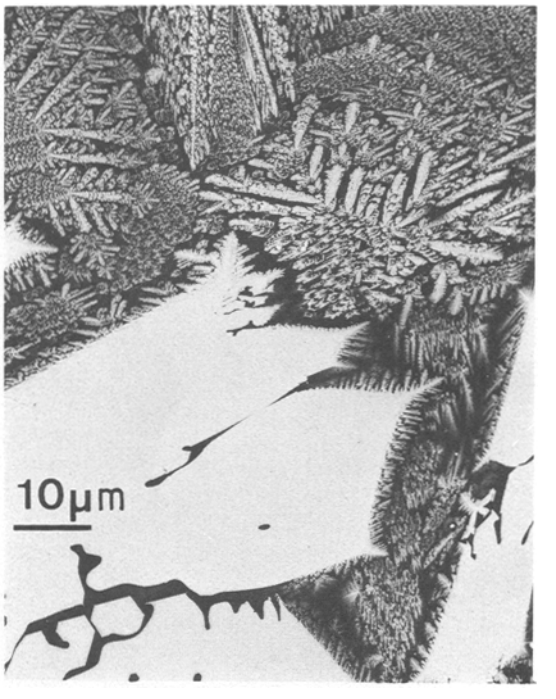

Figure 9 By annealing samples with a morphology of Fig. 8 at 1450° C, large crystals of willemite (bright) grow in a partial melt according to the ternary phase diagram (see discussion in the text).

gives rise to a decrease of the melting temperature until about 1400° C depending on the actual composition [7]. Hence, additional annealing of such samples at about 1300 and 1450° C yields different effects: Annealing at 1300° C for 6 to 9 h (i.e. at sub-solidus temperatures) provides larger regions of both phases *A* and *B*. By annealing at 1450° C for 3 h, however, partial melting takes place and phase *A* grows with a morphological habit as in its field of primary formation [9]. This growth process generates a morphological change from that of Fig. 8 to that of Fig. 9 which is observed besides unresolved primary *B*-crystals. Little enstatite is also present according to X-ray diffraction.

Prolonged annealing (> 5 h) at 1450° C produces even macroscopical softening and melting of the samples. The earlier observed [8] lower peritectic temperature of 1460° C may therefore also be due to the presence of small amounts of extra SiO_2.

The liquidus and solid lines of the regions I and II in Fig. 1 have been drawn tentatively. They can be checked by some approximate calculation using the equation [17]

$$\ln\left(\frac{X_Z^s}{X_Z^l}\right) = \frac{\Delta H_{f,Z}}{T_{f,Z}R} \cdot \frac{\Delta T}{T}$$

which describes the change of the melting temperature $\Delta T = T_{f,Z} - T$ of a compound Z in relation to the presence of a second component in the liquid melt. In this equation, X_Z^s and X_Z^l are the molar fractions of the compound Z in the coexisting solid and liquid phases, respectively, at the actual temperature T(K). $\Delta H_{f,Z}$ and $T_{f,Z}$ are, respectively, the enthalpy and temperature of fusion of the compound Z, and R is the gas constant. This equation has been shown earlier [18] to give reasonable agreement between experimental and calculated liquidus temperatures. Considering the experimental values of forsterite as Z with $X^s = 0.73$ (P3 in Fig. 1), $X^l = 0.28$ (P1) at the peritectic temperature $T = 1788$ K and $T_f = 2163$ K [16], the equation above yields $\Delta H_f \approx 19$ kcal mol^{-1}. This is in good agreement with the known values of ΔH_f of Fe_2SiO_4 and Mn_2SiO_4 (22.0 and 21.4 kcal mol^{-1}, respectively [16]) according to their crystallochemical relationship to Mg_2SiO_4. On the other hand, by use of the liquid

composition and the temperature of the earlier proposed eutectic [18], one obtains ΔH_f (Mg_2SiO_4) ≈ 7 kcal mol^{-1} which is far from those enthalpy values above.

In the same way, the observed lower melting temperature of zinc silicate with $\Delta T = -40°$ C below the peritectic temperature is confirmed by calculation using $X^s = 0.55$ (P2) and $X^l = 0.72$ (P1) at $T = 1788$ K as experimental values and assuming ΔH_f to be about 25 kcal mol^{-1}.

4. Conclusions

Zn_2SiO_4–Mg_2SiO_4 forms a peritectic system (Fig. 1), where the peritectic temperature (1515° C) is situated above the melting point of zinc silicate. At the peritectic temperature T_0, the coexisting melt (28% Mg_2SiO_4, P1) and forsterite solid solution (73%, P3) react with each other to form zinc silicate solid solution (45%, P2).

The formation of willemite from zinc-silicate-rich melts is influenced by kinetic factors: due to the loss of some ZnO at high temperatures, the exceeding SiO_2 and MgO is kept in the solid solution only during slow growth from the melt. The crystal lattice is then distorted. By subsequent annealing, MgO and SiO_2 is preferrently separated from the willemite solid solution. On the other hand, rapid growth from the melt gives rise to preferred exsolution of ZnO rather than MgO and SiO_2 at the grain boundaries of willemite.

From melts containing more than about 30% Mg_2SiO_4, primary forsterite solid solution forms above T_0 and reacts only sluggishly with the residual melt below T_0 under decomposition. During the growth of zinc silicate solid solution in the two-solid-phase field (III, Fig. 1), SiO_2 is more strongly enriched in the ambient regions than MgO and ZnO. Thus, a ternary phase assemblage forms with a melting temperature of ~1400° C [7] which can no longer be completely transformed to the pseudobinary phase assemblage.

Acknowledgements

We thank Professor H. R. Oswald for his stimulating interest in this work. Financial support by the Swiss Commission for the Encouragement of Scientific Research (Project Number 791.1) is gratefully acknowledged.

References

1. A. R. WEST and F. P. GLASSER, *J. Mater. Sci.* **6** (1971) 1100.
2. *Idem, ibid* 7 (1972) 895.
3. F. P. GLASSER, *Phys. Chem. Glasses* 8 (1967) 224.
4. A. R. WEST and F. P. GLASSER, *Mat. Res. Bull.* **5** (1970) 837.
5. E. N. BUNTING, *J. Res. National Bur. Standards* **4** (1930) 131.
6. J. WILLIAMSON and F. P. GLASSER, *Phys. Chem. Glasses* **5** (1964) 52.
7. E. R. SEGNIT and A. E. HOLLAND, *J. Amer. Ceram. Soc.* **48** (1965) 409.
8. J. F. SARVER and F. A. HUMMEL, *ibid* **45** (1962) 304.
9. L. WEBBER and H. R. OSWALD, *J. Mater. Sci.* **10** (1975) 973.
10. L. WEBBER, H. R. OSWALD and E. GRAUER-CARSTENSEN, *Micron* **6** (1975) 129.
11. L. WEBBER and U. EGLI, *J. Mater. Sci.* **12** (1977) 1981.
12. L. WEGMANN, *Microscopy* **96** (1972) 1.
13. L. WEBER and H. R. OSWALD, *Optik* **45** (1976) 333.
14. A. GAEUMANN, *Chimia* **20** (1966) 82.
15. A. GAEUMANN and J. OSWALD, *ibid* **21** (1967).
16. R. A. ROBIE and D. R. WALDBAUM, *Geol. Surv. Bull. USA* **1259** (1968) 213.
17. P. GARDON, "Principles of phase diagrams in materials systems", (McGraw-Hill, New York, 1968) p. 77.
18. S. A. SUVOROV and V. K. NOVIKOV, *Inorganic Mat.* 7 (1971) 246.
19. NBS Circular 539/7 (1957) 62 (ASTM 8-492).

Received 10 January and accepted 18 February 1977.